Extended Data

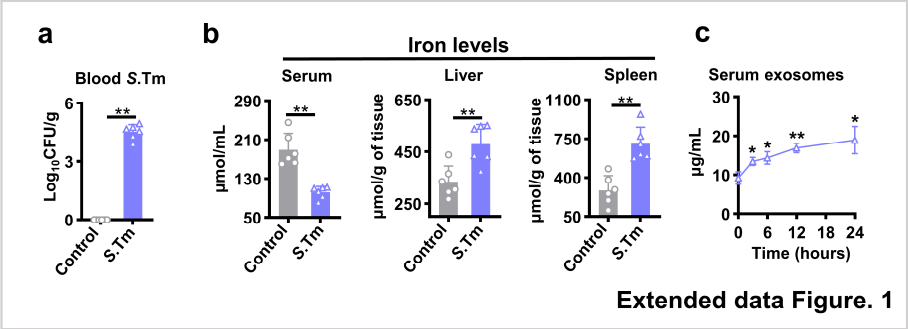

Extended Data Fig. 1 The establishment and characterization of *S*.Tm-infected mice.
(a-c) The C57BL/6J mice were intraperitoneally administrated with *S*.Tm, and blood and tissues samples were collected for further analysis. **a,** The viable counts of *S*.Tm in the blood at 24h after infection. n = 6 mice. **b,** Serum (left), hepatic (middle), and splenic (right) iron levels in mice at 24h after infection. n = 6 mice. **c,** The concentration of exosomes in serum within 24 hours after infection. n = 3 mice per time point. For **a-c**, data are presented as the mean ± s.d. For **a-c**, statistical significance was assessed by unpaired two-tailed Student's t test. *p < 0.05, **p < 0.01.

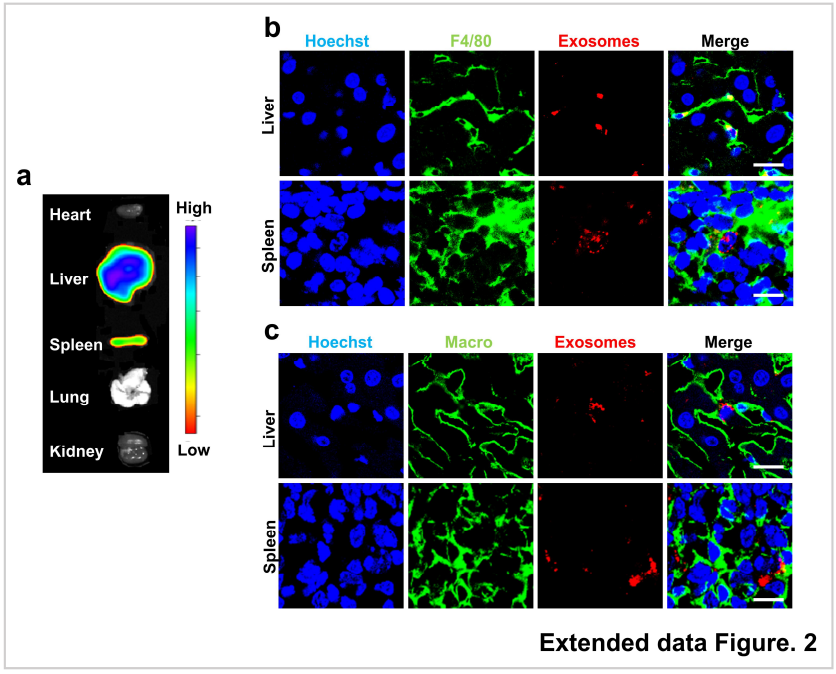

Extended Data Fig. 2 Serum exosomes were captured in liver and spleen *in vivo*.
a, *Ex vivo* fluorescence images of various organs in mice systemically injected with DiR-labeled serum exosomes. n = 3 mice. **b**, **c**, Confocal microscopy images showing the uptake of PKH26-labelled exosomes (red) by F4/80$^+$ cells (green) **(b)** or Macro$^+$ cells (green) **(c)** in liver or spleen.

Scale bar, 10 μm. n = 3 biologically independent samples.

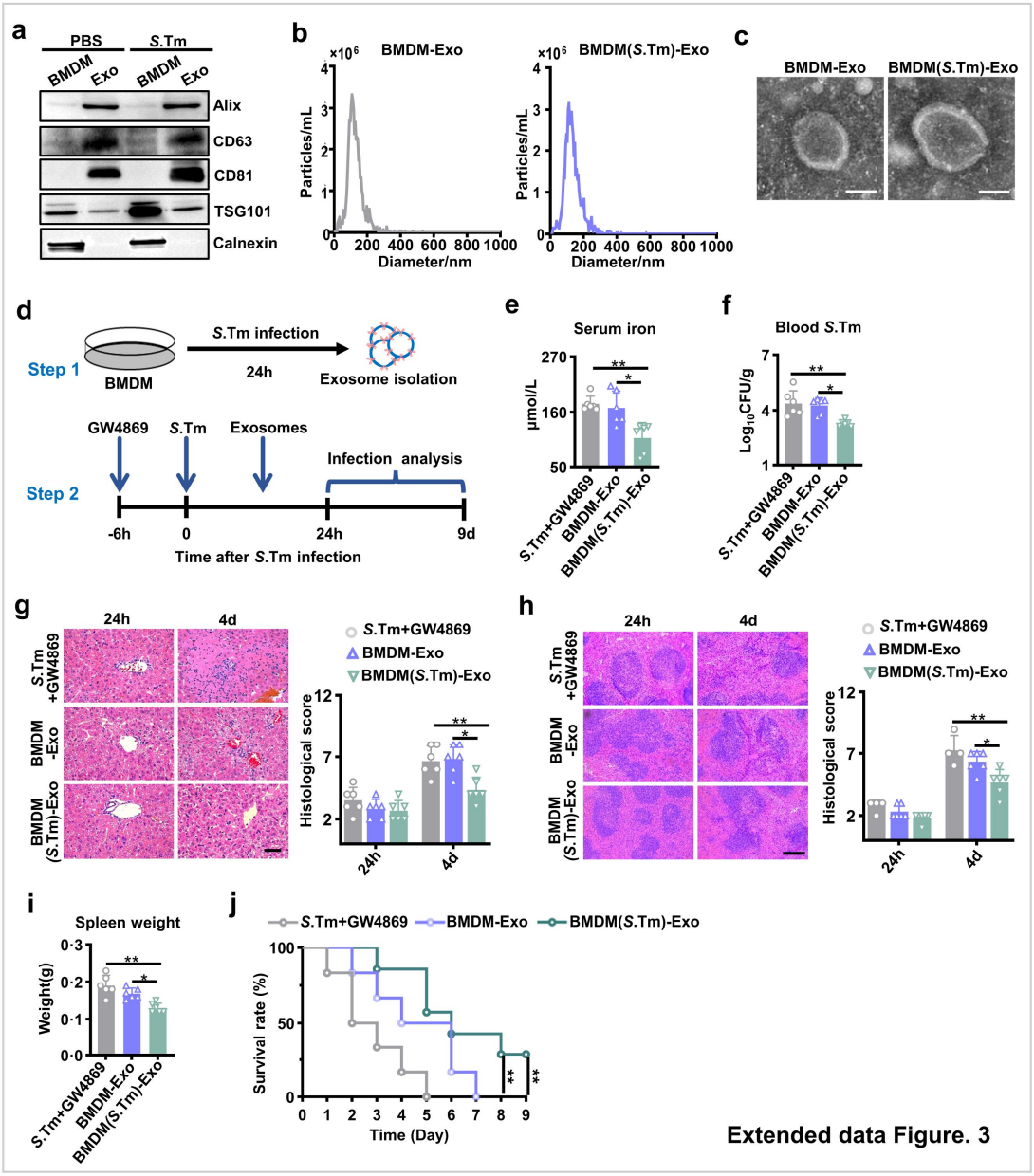

Extended Data Fig. 3 Supplementation with exosomes derived from BMDM decreases infection severity in exosome-deficiency mice.

(a-c), BMDM were infected with *S*.Tm for 24 hours at an MOI of 10. Exosomes were isolated from the uninfected BMDM (BMDM-Exo group) or *S*.Tm-infected BMDM [BMDM(*S*.Tm)-Exo group] and characterized. **a,** Western blot analysis of the exosome markers Alix, CD81, CD63 and TSG101 and the negative mitochondrial markers calnexin**. b,** NTA analysis of the concentration and size distribution of exosomes**. c,** TEM images of exosomes, scale bar, 50 nm. **d,** Schematic diagram of the experimental procedure. Exosomes were isolated from uninfected BMDM or *S*.Tm-infected BMDM (Step 1). To investigate the role of host exosomes in iron metabolism and infection

outcomes, GW4869-pretreated *S*.Tm-infected mice were intravenously injected with exosomes derived from uninfected BMDM (BMDM-Exo group) or *S*.Tm-infected BMDM (BMDM (*S*.Tm)-Exo group), and the mice were euthanized after 24 hours for further analysis (Step 2). **e,** The iron levels in serum. n = 6 mice. **f,** Viable count of *S*.Tm in blood. n = 6 mice. **g, h,** Representative H&E staining of the liver **(g)** and spleen **(h)** at 24 hours or day 4 after *S*.Tm infection and quantitative analysis of histological scores. scale bar, 50 μm **(g)** and 250 μm **(h)**. n = 6 mice**. i,** Quantitative analysis of the spleen weights at day 4 after infection. n = 6 mice. **j**, Survival rate of mice. n = 6 mice. For **e-i**, data are presented as the mean ± s.d. For **f**, **g-i,** statistical significance was assessed by one-way ANOVA with Tukey's post-hoc test. For **e,** statistical significance was assessed by the Kruskal-Wallis test. For **j,** statistical significance was assessed by the log-rank test. *p < 0.05, **p < 0.01, ns, not significant.

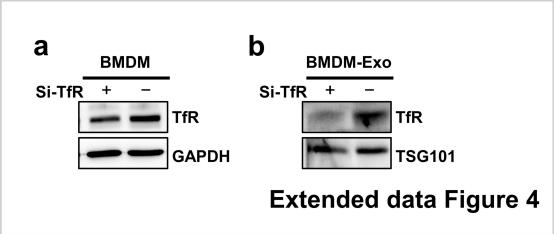

Extended Data Fig. 4 Inhibition of the TfR expression in BMDM and BMDM-derived exosomes via siRNA.

a, Western blot analysis of TfR in BMDM transfected with TfR siRNA. **b**, Western blot analysis of TfR in exosomes derived from BMDM transfected with TfR siRNA.

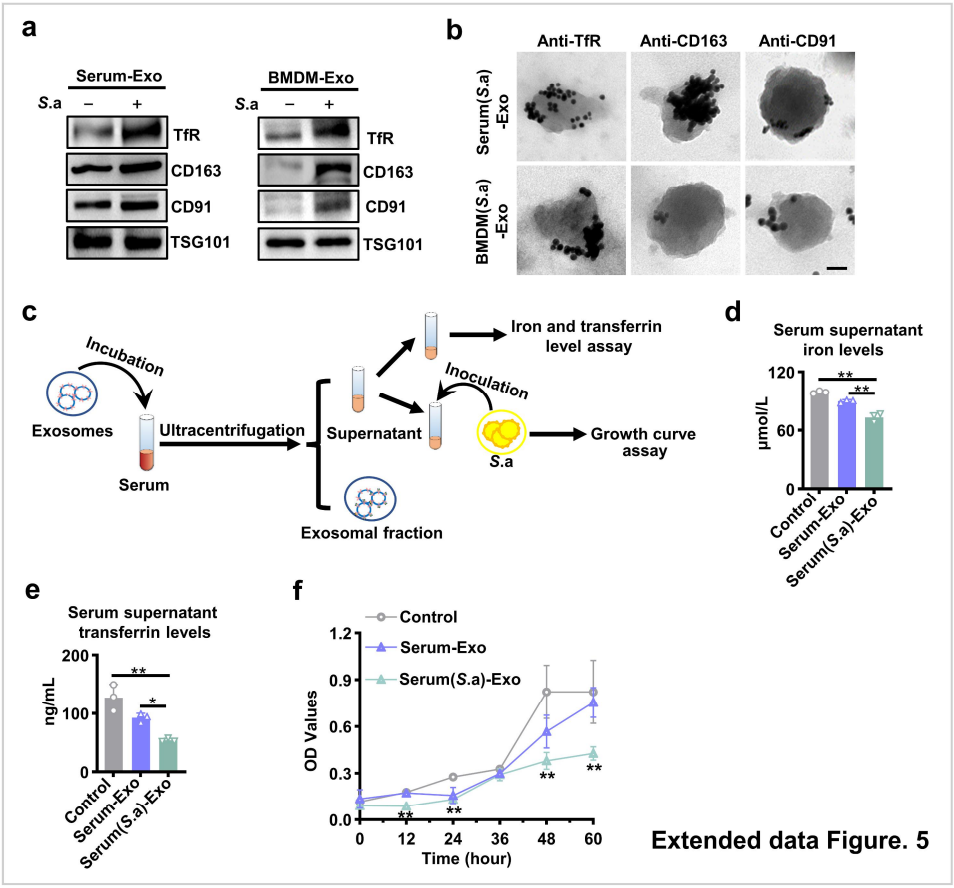

Extended Data Fig. 5 TfR-, CD163-, CD91-bearing exosomes derived from *S*.a-infected mice or BMDM bind iron.

(a-c), Normal mice was intraperitoneally injected with *S*.a and the serum were collected after 24 h. BMDM were infected with *S*.a for 24 hours at an MOI of 25 and supernatant was collected. Exosomes were isolated from the serum or supernatant. **a,** Western blot analysis of TfR, CD163, CD91 and TSG101 expression in exosomes derived from uninfected and infected mouse serum (left), and in exosomes released from uninfected or infected BMDM (right). **b,** Immunoelectron microscopy detection for TfR, CD163, and CD91 antibodies in exosomes derived from infected mouse serum (upper) or infected BMDM (bottom). Scale bar, 50 nm. **c**, Schematic diagram of the overall design of the experiments to test the ability of exosomes to bind iron in serum. Exosomes derived from uninfected mouse serum (Serum-Exo group) or *S*.a-infected mouse serum [Serum (*S*.a)-Exo group] were added to the serum respectively and incubated for 12 hours and then removed by ultracentrifugation. The serum supernatant was collected for further analysis. **d,e**, Total iron levels **(d)** and transferrin levels **(e)** in the serum supernatant after incubation with exosomes derived from uninfected or infected mouse serum. n = 3 biologically independent samples. **f,** Growth of *S*.a in serum supernatant. n = 5 biologically independent samples. For **d-f**, data are presented as the mean ± s.d. For **d** and **e,** statistical significance was assessed by one-way ANOVA with Tukey's post-hoc test. For **f,** statistical significance was assessed by one-way ANOVA with Tukey's post hoc test and Kruskal-Wallis test. *$p < 0.05$, **$p < 0.01$, ns, not significant.

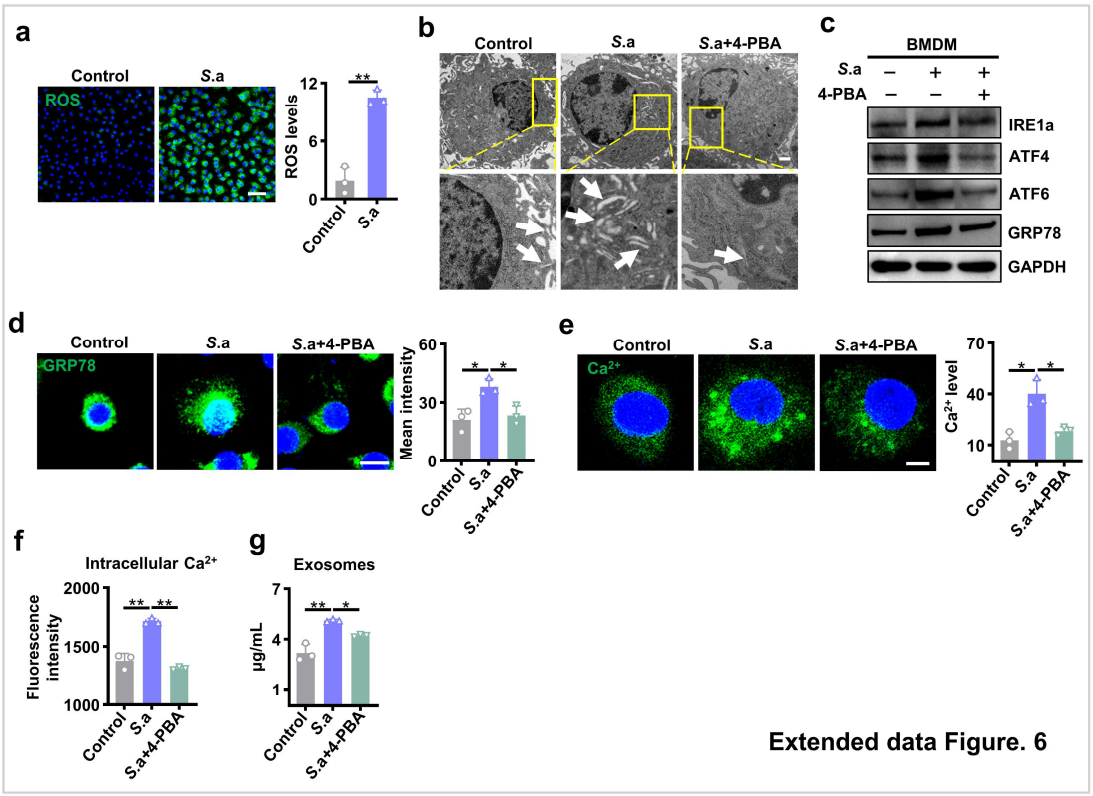

Extended Data Fig. 6 *S*.a infection induces exosome release via endoplasmic reticulum stress. **a,** Representative fluorescence images of ROS in BMDM infected with *S*.a at MOI of 25, and quantitative analysis of the ROS levels in cells. Scale bar, 50 μm. n = 3 biologically independent samples. **(b-g)**, BMDM were infected with *S*.a in the absence or presence of 4-PBA to clarify the association between ERS and exosome release. **b,** TEM images showed the ultrastructural morphology of the endoplasmic reticulum in BMDM. Scale bar, 1 μm. High-magnification images of the area marked by yellow boxes are arrayed at the lower panel. White arrow indicated endoplasmic reticulum. **c,** Western blot analysis of the expression of IRE1α, ATF4, ATF6 and GRP78 in BMDM. **d,** Representative fluorescence images of GRP78 in BMDM, and quantitative analysis of the fluorescence intensity Scale bar, 10 μm. n = 3 biologically independent samples. **e,** Representative fluorescence images of intracellular Ca^{2+} level in cells, and quantitative analysis of the Ca^{2+} levels. Scale bar, 4 μm. n = 3 biologically independent samples. **f,** Intracellular Ca^{2+} levels measured by fluorescence intensity. n = 3 biologically independent samples. **g,** The concentration of exosomes in supernatant. n = 3 biologically independent samples. For **a** and **d-g**, data are presented as the means ± s.d. For **a**, statistical significance was analyzed by unpaired two-tailed Student's t test. For **d-g**, statistical significance was analyzed by one-way ANOVA with Tukey's post-hoc test. *$p < 0.05$, **$p < 0.01$, ns, not significant.

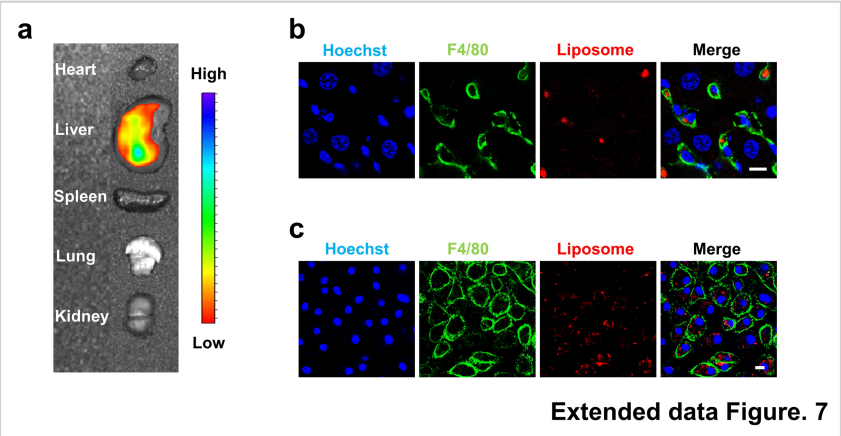

Extended Data Fig. 7 The biodistribution of 4-PBA-encapsulated liposome.

a, *Ex vivo* fluorescent images of various organs in mice injected with RhB-labeled 4-PBA-encapsulated liposome. n=3 mice. **b**,**c**, The uptake of RhB -labelled liposome (red) by macrophages in liver **(b)** or *in vitro* cultured BMDM (**c**) stained with Hoechst (nucleus; blue) and F4/80 (cell membrane; green). Scale bar, 10μm. n = 3 biologically independent sample.

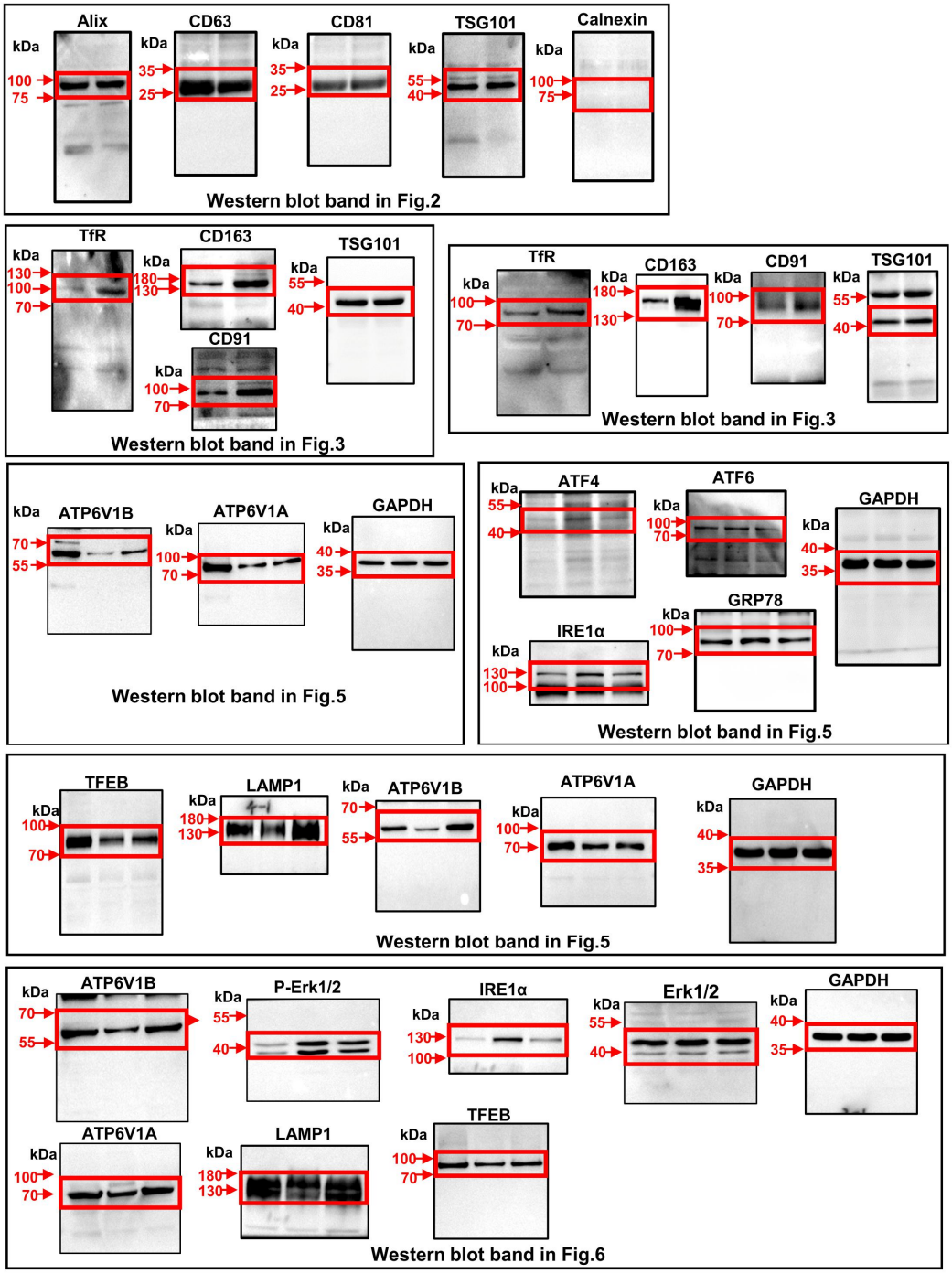

Extended data Figure 8

Extended Data Fig. 8 Uncropped Western blot bands.

Uncropped western blot bands for Figure 2, Figure 3, Figure 5, Figure 6.

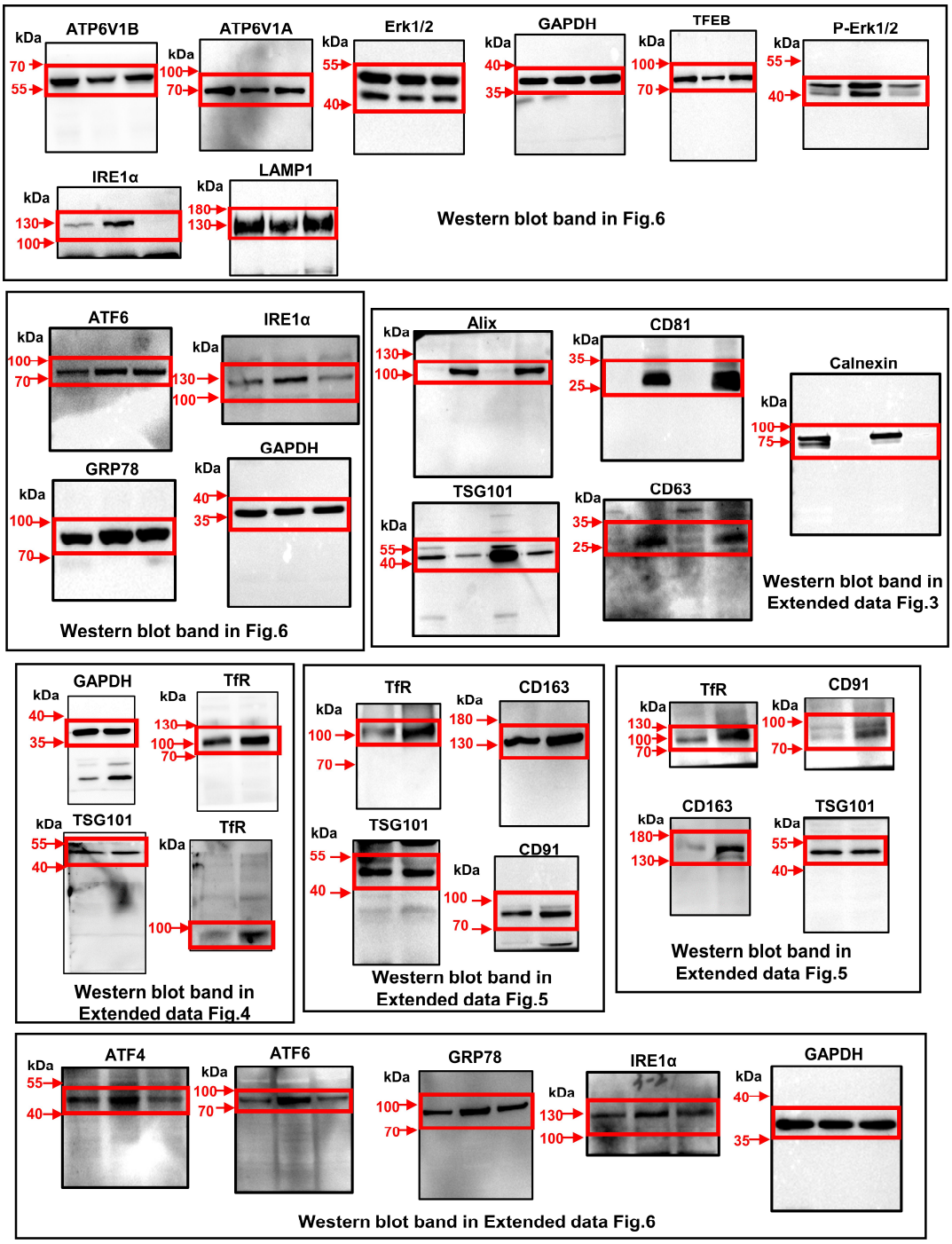

Extended data Figure 9

Extended Data Fig. 9 Uncropped Western blot bands.

Uncropped western blot bands for Figure 6, Ext. Figure 3, Ext. Figure 4, Ext. Figure 5, and Ext. Figure 6.